Adv Syst Sci Appl 2023; **03**:139–152
Published online at https://ijassa.ipu.ru.

Accurate Indoor Positioning System Based on Visible Light

Asmaa Hadjer Saboundji*, Mokhtar Keche, Mohammed Dahmani

Laboratoire Signaux et Images, Université des Sciences et de la Technologie d'Oran Mohamed Boudiaf (USTO-MB), El M'Naouar-Bir el Djir-Oran, Algeria

Abstract: Besides its use in high-rate wireless communications, visible light has recently emerged as an interesting positioning technology, which is referred to as Visible Light Positioning (VLP). Its main advantage is its high positioning accuracy. Like with other positioning technologies, many techniques may be used with VLP, such as Received Signal Strength (RSS), (Difference) Time Of Arrival ((D)TOA), Angle of Arrival (AOA), etc. In this paper, we investigate the use of the RSS technique for VLP. Two new methods are proposed and their performances are compared experimentally to those of three methods from the literature. Both of the proposed methods are based on polynomial fitting. The obtained results show that the second one has a positioning accuracy that is comparable to that of the best method among these three reference methods, while being simpler. It should be highlighted that with only standard low-cost commercial components relationship with, we could obtain a very high positioning accuracy, with a mean localization error in the order of 1 cm.

Keywords: indoor positioning, visible light positioning, RSS, machine learning, neural networks

1. INTRODUCTION

The localization of people or objects has become an essential part of the deployment of services in many fields, such as retail, logistics, urban planning, leisure, etc. The success of global positioning systems (GPS) and the mobile revolution have forever changed our relation to technology, both in business and in our personal lives. GPS cannot be used inside buildings because of the high-power attenuation, the multipath phenomena, and the low signal penetration [20]. Many technologies have been proposed for indoor location, such as: WiFi [28], Bluetooth [24], radio frequency identification (RFID) [9], ZigBee [5], and Visible Light [18]. The latter technology relies on the use of a Light-Emitting Diode (LED), which is a promising light source, due to its low energy consumption. Besides this, compared to traditional light sources, LEDs have many advantages, including brightness efficiency and long service life. In addition to lighting purposes, LEDs can also be easily modulated at relatively high data rates for data communications [18] . Such a technology is called Visible Light Communication (VLC). They also can be used for Visible Light Positioning (VLP). VLP is considered as an alternative solution for indoor positioning since it does not suffer from radio or electromagnetic interference. It has potential advantages such as cost reduction, durability, and environmental friendliness, but above all, from the point of view of localization, systems based on visible light have the capacity to estimate the position of an object with high precision [36]. There are several VL-based positioning methods, which can be classified into two categories according to the type of receiver [2]: the photodiode-based methods and the camera-based methods.

*Corresponding author: asmaahadjar.saboundji@univ-usto.dz

Camera based VLP refers to the use of an image sensor as a terminal for the positioning receiver; it is preferred in commerce and industry because of its high positioning accuracy [6]. In a VLP system, a camera is used to capture LED images. Then, the position of the receiver is determined based on the relationship between the known 3D coordinates of the LEDs in a real-world plane and their 2D coordinates in the image plane [11]. A lot of work has been done both for LEDs identification in the image plane and positioning. A camera based positioning system, which uses triple, or double LEDs is proposed in [7]; it achieves a centimeter accuracy. Another real-time VLP method, which uses double LEDs, with a lightweight image processing algorithm, is proposed in [19]; it achieves a 3.93 cm positioning accuracy. ZHANG et al. proposed in [33] a single LED VLP method, which exploits the property of circular projection and uses the geometric characteristics of the LED image to determine the position and orientation of the receiver with respect to the LED lamps reference plane. The average positioning error is reported to be 17.52 cm. In [16], an angle-of-arrival localization algorithm that uses a camera and three or more LEDs is proposed; it can achieve decimeter-level accuracy. Although VLP-based camera localization methods can achieve decimeter or even centimeter accuracy, they require expensive sensors and complex image processors [23]. On the other hand, PD-based positioning methods have a wide range of applications in the indoor positioning field due to the high sensitivity of a PD to the light, its low price, and the possibility of high reception bandwidth. PD-based positioning systems are generally based on multilateration or triangulation, which requires the calculation of the distance or angle between the emitter and the receiver. Many techniques have been developed for this purpose, such as the Time Of Arrival (TOA), the Time Difference Of Arrival (TDOA), Angle Of Arrival (AOA), and Received Signal Strength (RSS).

TOA or TDOA is an important technique in localization, which is used in GPS [17]. It requires highly synchronized hardware, which increases the implementation costs [14]. In TOA, the absolute travel time of a wireless signal from the transmitter to the receiver is first estimated [3]. Knowing the speed of propagation of light, the TOA measurement allows measuring the distances between the transmitters and the receiver, which are then applied to a trilateration method to determine the position of the receiver. This makes the TOA technique difficult to implement because it requires precise synchronization between the transmitters and the receiver. Therefore, to avoid the need for precise time synchronization, indoor location systems generally opt for TDOA rather than TOA, because TDOA requires synchronization between transmitters only, which is easier to achieve [21]. However, while TDOA methods could be an appropriate solution with some technologies, they are not an optimal choice for economic LED indoor positioning, because the differences in the traveling times of the signals are too short, due to the short distances between the transmitters and the receiver, which requires highly accurate and synchronized clocks to estimate them.

The Angle of Arrival (AOA) is defined as the angle between the propagation path of a wave (its incidence) and a reference direction [22]. Geometrically, AOA localization consists of finding a point in 3D space so as to minimize the sum of the distances between this point and the lines drawn between the LED transmitters and the receiver [4,25,27]. AOA technique can provide high accuracy with an expensive sensor array, such that the measured angles are not limited by the receiver's field of view. Therefore, RSS-based methods are the most common for indoor VLP, since they do not require synchronization, which reduces the cost and complexity of implementation [26]. In addition, RSS values are easy to obtain using a photodetector and a simple power measurement algorithm [37].

Many research works have been carried out for RSS based indoor VLP. Jung et al, [13] proposed a localization technique using the received signal strength ratio (RSSR), which is the relative ratio of optical powers detected between each LED and optical receiver. Three equations could be obtained using the force ratio between the received signals, and the position of the terminal is located by solving these equations. In [34]a positioning system, by varying the transmission power, was proposed in order to estimate the distances to several light sources, however, this leads to unstable lighting. Yang et al [29] also

presented a localization method, which uses a single transmitter and multiple receivers, whose center is determined using their RSS and the relative positions between them. An average positioning error of 0.65 cm was reported. However, the implementation of the method is not straightforward and requires equipping the mobile device with three receivers that are deployed in fixed positions, relatively to each other. In [31], a positioning error lower than 3 cm has been reported in 3-D localization, however, besides the light sensor, an extra accelerometer or gyro-sensor is required by the system, which increases the positioning algorithm complexity. Yang [30] proposed a 3-D indoor positioning system using AOA and RSS with a single transmitter and multiple optical receivers. They showed that the positioning error is less than six cm. [12] puts forward an indoor 3-D visible light fingerprint positioning system based on the fusion of a K-means algorithm and a RF algorithm. The reported average 3-D location error is 4.45 cm. In [8], Chin-Wei Hsu et al. proposed to subdivide the entire positioning zone into several small sub-zones, and in each sub-zone, they applied a positioning algorithm that directly estimates the mobile's position from the RSS. The two coordinates of this position are estimated separately and each of them is expressed as a quadratic polynomial of the powers received from four LEDs. The coefficients of this polynomial are determined during a training phase by what they called "machine learning", which in fact uses the steepest descent algorithm to find the solution. Artificial Neural Networks (ANN) have also been proposed for estimating the position of a receiver directly from the RSS. For example, the authors in [10] trained a typical back-propagation ANN with the RSS received from four LEDs at different points on the receiver plane to learn the relation RSS-position, then the trained ANN is used to retrieve the position of the receiver from the four RSS during the operational phase.

This paper, proposes two new visible light-based positioning methods. The performances of these methods are assessed experimentally and compared to that of some other methods from the specialized literature. The rest of this paper is organized as follows: The system model for indoor positioning is described in section. 2. Section. 3 presents the proposed two VLP methods. In section 4, the experimental results are presented and discussed. Finally, in section 5, some conclusions are drawn.

2. INDOOR POSITIONING CHANNEL MODEL

As shown in Figure 2.1, a typical indoor scenario with four LEDs and a photodetector is considered in this paper. In RSS-based VLP, the position of the mobile device (receiver) is determined by a location algorithm, from the strength of the signals received from LEDs. The LED is often considered as a Lambertian source [1, 15]. Therefore, when only the line-of-sight (LOS) channel is considered, the distance between a LED and the receiver can be estimated by measuring the received signal power, which can be expressed by:

$$P_r = \begin{cases} \frac{(m+1)A\cos^m(\phi)\cos(\theta)}{2\pi d^2} T(\theta) g(\theta) P_t & 0 \leq \theta \leq FOV \\ 0 & \theta > FOV \end{cases} \tag{2.1}$$

where

- P_t is the transmitted power,
- A is the physical area of the detector in the PD,
- ϕ and θ are, respectively, the irradiance angle and the incidence angle, as shown in Figure 3.2,
- $T(\theta)$ is the gain of the optical filter,
- $g(\theta)$ is the gain of the optical concentrator,
- FOV is the field of view at the PD,
- d is the distance between the LED and receiver,
- m is the Lambertian mode number related to the semi-angle at half-power of the LED, $F_{1/2}$, by:

$$m = \frac{-\ln 2}{\ln(\cos F_{1/2})} \tag{2.2}$$

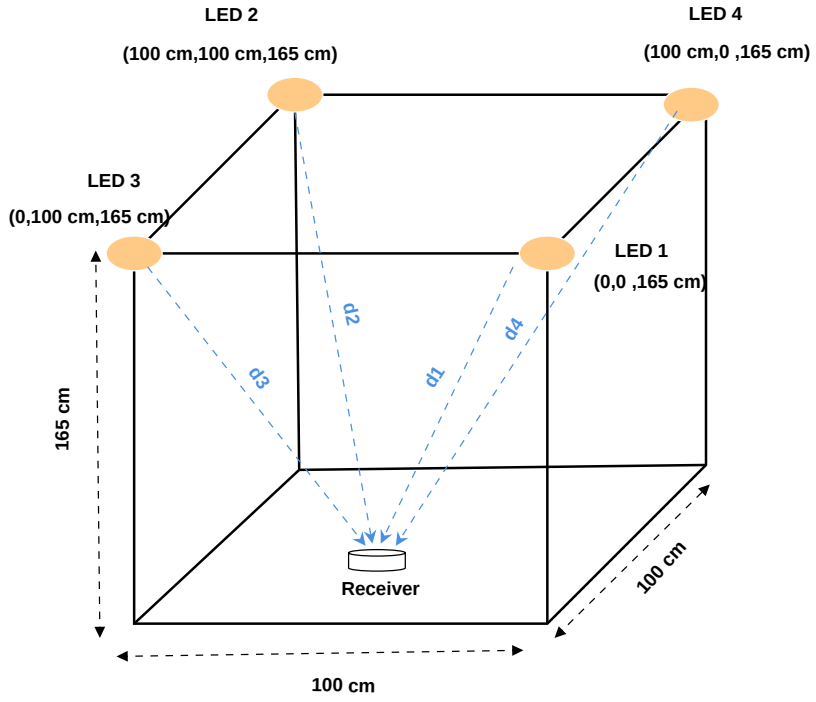

Fig. 2.1. Scenario considered for visible light positioning

3. THE VLP PROPOSED METHODS

In the following, we describe the two proposed VLP methods. Both methods are based on polynomial fitting. In the first method, the relation distance-RSS is expressed by a polynomial

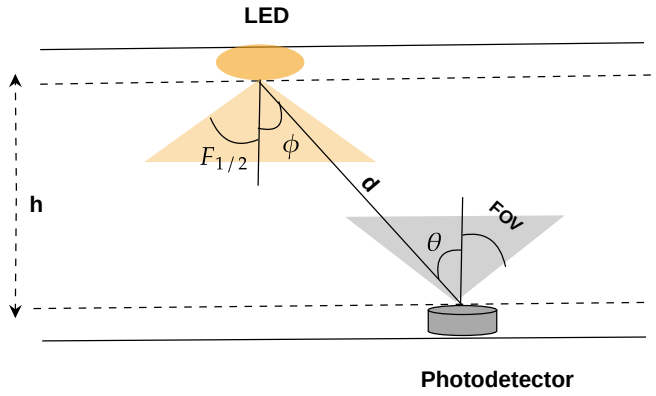

Fig. 3.2. Parameters of the optical wireless channel

whose coefficients are determined by a polynomial fitting method, during a training phase.

This relation is then used during the operational phase to retrieve the distances between the receiver and at least three emitters (sources), from the powers of the signals received from these emitters. Once the distances are determined, they can be used to estimate the position of the receiver, by applying a multilateration method.

In the second method, the coordinates of the receiver are directly expressed as a function of the received powers. This function is assumed to be a polynomial, whose parameters are determined using polynomial surface fitting.

3.1. The first proposed method

As we have seen in the previous section, the RSS is related to the distance between the emitter and the receiver. A usual approach is to model the relation distance-power, during an offline training phase, then use this relation to retrieve the distance from the RSS, during the operational phase. Once the distances between a receiver and at least three emitters, or an emitter and at least three receivers are estimated, trilateration can be applied to estimate the position of the mobile device.

Many models have been proposed in the related literature to express the received power-distance relation. For example, the following relation was proposed in [35] .

$$P_r^i / P_0^i = \frac{h}{d_i^n} \tag{3.3}$$

where:

- P_r^i is the power received form led i,
- P_0^i is a reference power, i.e. the power received form led i at a given reference point,
- h is the vertical distance between the emitters and the receiver,
- d_i is the distance between led i and the receiver,
- n is a parameter whose value can be determined experimentally by applying a non-linear fitting to a set of training measurements.

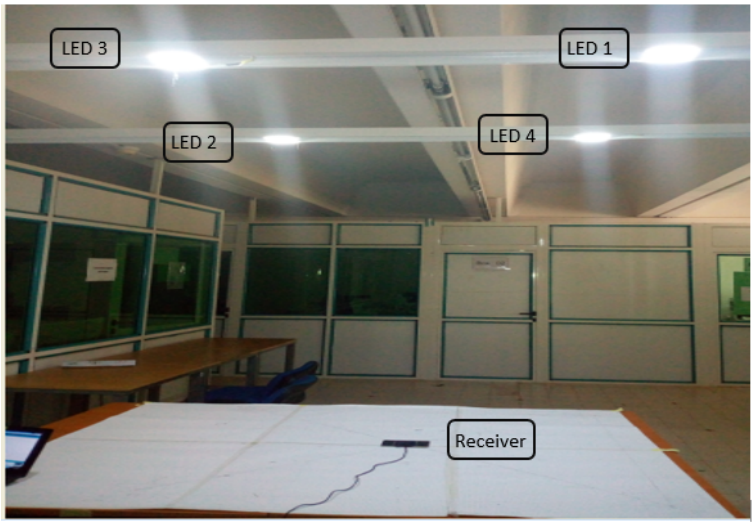

Fig. 3.3. Experimental test bed

In the following, this fitting will be denoted the Simplified Lambertian Fitting. For a better fitting, we assume in this paper that the relation distance-power is polynomial. We have investigated the use of polynomial curve fitting, which is probably one of the simplest

and most used data fitting techniques. In this fitting, the relation distance-power is expressed as follows:

$$d = \sum_{k=0}^{n} c_k p^k \tag{3.4}$$

where d is the distance, p is the power, c_k is the k^{th} coefficient of the polynomial and n is its degree. To determine the coefficients c_k, we first carried out a measurement campaign during which the powers received from a given LED were measured at different points located on a square grid. Then, knowing the distances of these points to that LED, we applied a polynomial fitting method to obtain the coefficients c_k. This is achieved offline during what is called a training phase. During the operational phase, relation 3.4 is used to estimate the distances of the receiver to the sources from the powers of the signals received from these sources. These distances are then inputted into a multilateration method to estimate the position of the receiver. This method solves the following system of non-linear equations:

$$\begin{cases} (x-x_1)^2 + (y-y_1)^2 & = d_1^2 \\ (x-x_2)^2 + (y-y_2)^2 & = d_2^2 \\ & \vdots \\ (x-x_n)^2 + (y-y_n)^2 & = d_n^2 \end{cases} \tag{3.5}$$

where n is the number of sources, (x, y) are the coordinates of the receiver, (x_i, y_i) are the coordinates of the i^{th} source, and d_i is the distance between the receiver and the i^{th} source. By Using linearization and the least squares estimation, it can be shown that the position may be obtained as follows [32]:

$$\begin{bmatrix} x \\ y \end{bmatrix} = \frac{1}{2}(A^T A)^{-1} A^T B \tag{3.6}$$

where:

$$A = \begin{bmatrix} (x_2 - x_1) & (y_2 - y_1) \\ \vdots & \vdots \\ (x_n - x_1) & (y_n - y_1) \end{bmatrix} \tag{3.7}$$

$$B = \begin{bmatrix} x_2^2 - x_1^2 + y_2^2 - y_2^2 + d_2^2 - d_1^2 \\ \vdots \\ x_n^2 - x_1^2 + y_n^2 - y_1^2 + d_n^2 - d_1^2 \end{bmatrix} \tag{3.8}$$

3.2. The second proposed method

In this method, each of the two coordinates of the receiver is modeled separately as a polynomial of the received powers whose coefficients are determined by using surface polynomial fitting. In order to use available methods for this purpose the coordinate x or y is expressed as a function of only two received powers. If we denote these two powers by p_1 and p_2, then the coordinate x is approximated by:

$$\hat{x} = c_{0,0} + c_{1,0}p_1 + c_{0,1}p_2 + \cdots + c_(i,j)p_1^i p_2^j + \cdots \tag{3.9}$$

A similar relation is used for the y coordinate.

Notice that since only two powers are used in relation 3.9, the solution is not unique. In fact, there are two solutions that correspond to the intersections of two circles, centered, respectively on the first and second emitters with radii equal, respectively, to the distances between the receiver and these two emitters.

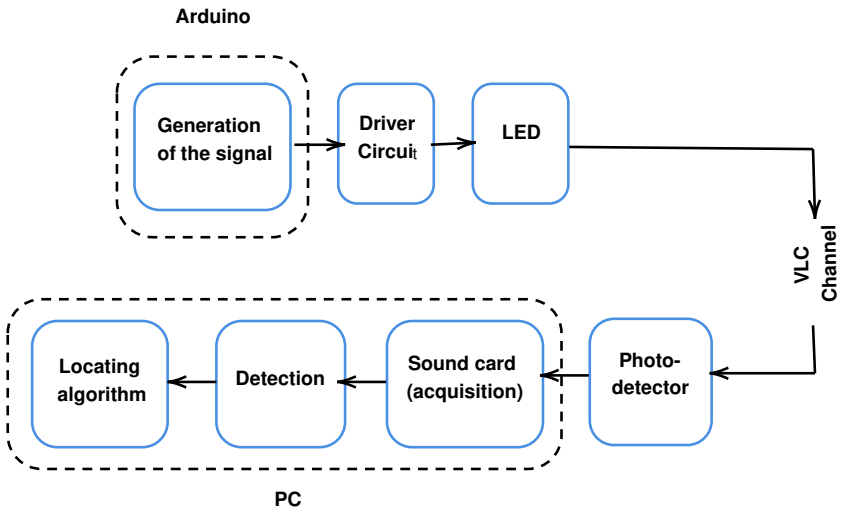

Fig. 3.4. Diagram of the constructed experimental VLP system.

Therefore, for each couple of powers (emitters), two couples of relations should be established, one for the points that represent the first solution, and one for the points that represent the second solution. This implies that the training set should be split into two non-overlapping sub-sets; the first one is used for the first relation and the second one for the second relation.

If n emitters are used, then in total $2c_n^2$ couples of relations should be used and thus the same number of solutions is obtained. Since only half of these solutions are valid, a pruning method can be applied to exclude the outsiders and average the remaining solutions to get an estimate of the true position.

4. EXPERIMENTAL RESULTS AND DISCUSSION

To evaluate the performances of the proposed VLP methods, many experiments were carried out using a test bed that has been built up for this purpose. Before presenting the obtained results and discussing them, we first present the experimental environment.

4.1. Experimental environment and parameters

A photo of the constructed test bed is shown in Figure 3.3. It consists of four low-consumption commercial LED lamps that are fixed on a ceiling at emplacements, as indicated in Figure 2.1, an emitter circuit, and a receiver circuit (see Figure 3.4). The emitter circuit is composed of an Arduino card that generates four signals; each signal controls the lightening of a LED lamp through a driver circuit. In order to discriminate the signals received from the LEDs, the lights emitted by these LEDs are modulated at different frequencies, which are respectively, 800 Hz, 900 Hz, 1000 Hz, and 1100 Hz.

The receiver includes a photo resistance, which is displaced horizontally at a distance of 165 cm from the ceiling, and a PC. The received signal is acquired by the sound card of the PC at a sampling frequency equal to 96 KHz. The digitized signal is then applied to a detection algorithm that uses the FFT to compute the powers of the four frequencies, i.e. the powers of the signals received from the four LEDs. These powers are then applied to a locating algorithm to determine the position of the mobile, i.e. the photo resistance.

The following five locating algorithms were implemented and tested:

- the two proposed in the present paper,
- the one proposed in [8] and named “machine learning (ML)method”,

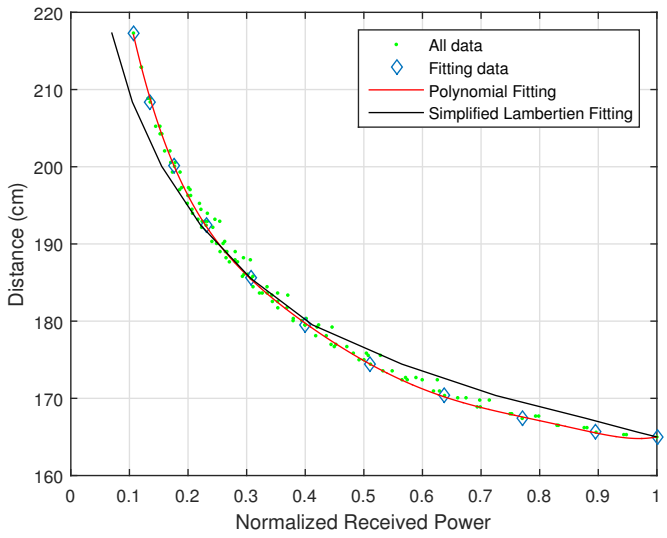

Fig. 4.5. Comparison between the polynomial fitting and the simplified Lambertian fitting

- the locating algorithm proposed in [10], which is based on Neural Networks,
- the one that uses multilateration and the Simplified Lambertian Fitting (SLF) to estimate the distances from the powers [35].

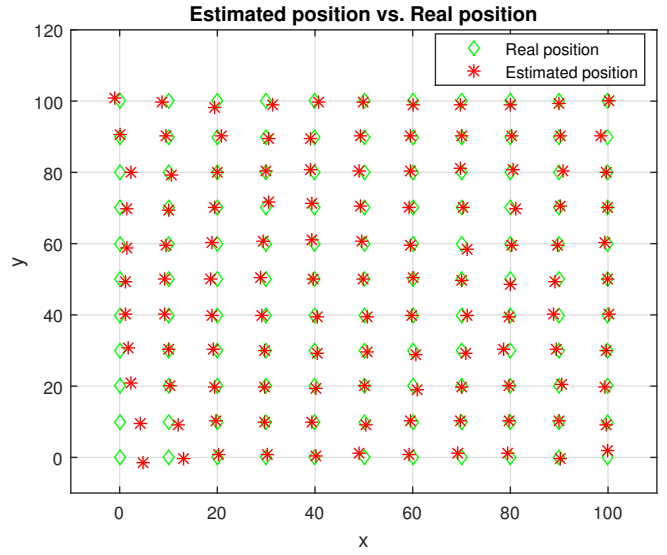

Fig. 4.6. Training results for the second proposed method (surface fitting)

All of the five methods cited above require learning. For this purpose, a training phase was conducted during which 121 normalized measurements were collected and stored in a file. Each measurement consists of the four powers received from the four LEDs at a given point, which is located on a uniform square grid that covers the (100cm x 100cm) positioning zone, whose origin, (0cm, 0cm), is taken to be the projection of the center of the first LED lamp. To test the generalization of the learning, two test files were used.

The first test file contains 121 normalized power measurements collected at the same points as during the training phase, whereas the second test file stores 121 normalized power

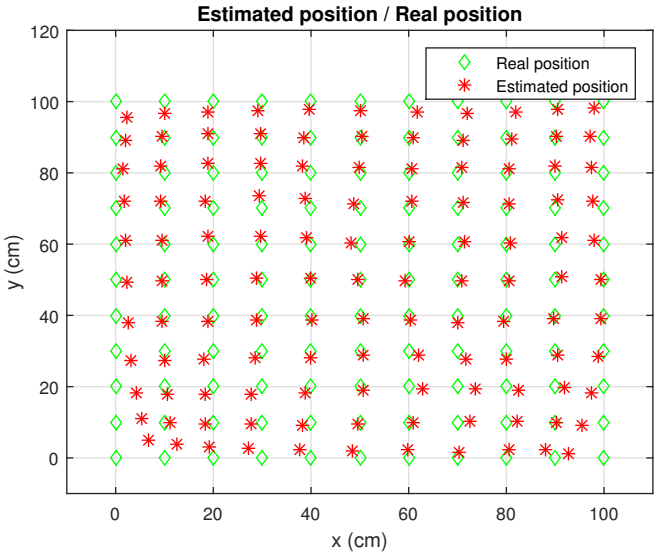

Fig. 4.7. Training results for the machine learning method

measurements, collected at points situated on a uniform square grid whose origin is (5 cm, 5 cm). Notice that the measurements in the learning file and the two test files were acquired at different dates.

4.2. Experimental Results Analysis

First, let us present the results of the training. Figure 4.5 compares the polynomial fitting used in the first proposed method and the simplified Lambertian fitting proposed in [35].

For the polynomial fitting, a degree six was found to be sufficient. It should be mentioned that only the 11 measurements lying along the diagonal that connect the points (0 cm, 0 cm) and (100 cm, 100 cm) were used for both fittings. From this figure, it can be observed that the polynomial fitting is more precise.

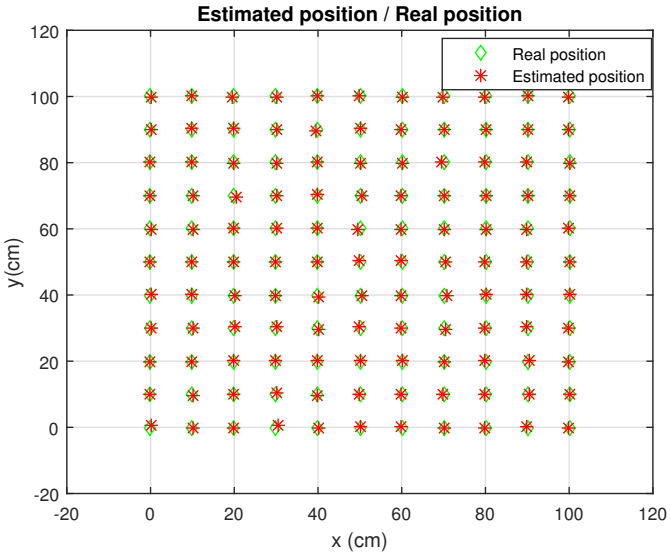

Fig. 4.8. Training results for the ANN method

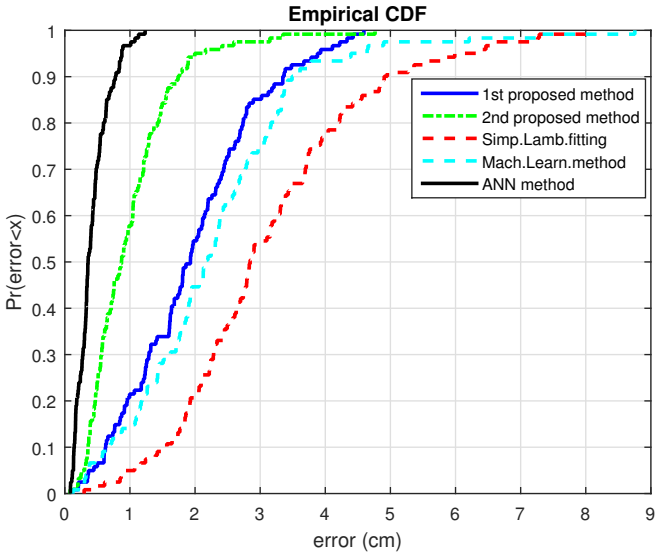

Fig. 4.9. CDF of the positioning errors obtained with the five VLP methods, using test file 1

For the proposed surface fitting method, the machine learning method [8] and the ANN method [10], the whole 121 measurements were used for training. For the surface fitting method, a polynomial of degree 3 in both variables was found to give the best results. For the machine learning method, the least squares method was employed to compute the parameters of the model. For the ANN method, a network with 10 hidden layers was trained using the backpropagation algorithm, with Bayesian regulation. The learning results for these three methods are presented in Figures 4.6, 4.7, and 4.8, where the true positions and the estimated ones are plotted together. These figures show that the ANN has the lowest training

Table 4.1. Position errors' statistics obtained with the five VLP methods, using test file 1

Method	Errors (cm)			
	Min	Mean	90%	Max
ML [8]	0.12	2.27	3.50	8.47
ANN [10]	**0.05**	**0.43**	**0.78**	**1.15**
SLF [35]	0.30	3.13	4.90	8.00
First proposed method	0.02	2.06	3.37	4.39
Second proposed method	0.10	0.91	1.47	3.42

error, followed by the surface fitting method, followed by the machine learning method. The obtained mean position errors are respectively, 0.24 cm, 0.79 cm, and 2.23 cm.

The results obtained by the five implemented VLP methods with test file 1 are summarized in Table 4.1 and Figure 4.9, whereas those obtained with test file 2 are summarized in Table 4.2 and Figure 4.10. In the tables, some statistics of positioning errors are reported, while the figures display the Cumulative Distribution Function of these errors. The positioning error is defined by:

$$e = \sqrt{(x_t - x_e)^2 + (y_t - y_e)^2} \tag{4.10}$$

where (x_t, y_t) and (x_e, y_e) denote, respectively, the true position and the estimated position.

From these results, it can be observed that to different extents the generalization in the five compared VLP methods is good enough. The best results were obtained with the ANN method, whereas the worst results were obtained with the method that uses the simplified

Table 4.2. Position errors' statistics obtained with the five VLP methods, using test file 2

Method	Errors (cm)			
	Min	Mean	90%	Max
ML [8]	0.23	2.81	5.35	8.72
ANN [10]	**0.04**	**1.29**	**2.70**	**4.07**
SLF [35]	0.16	3.25	5.34	9.65
First proposed method	0.06	2.49	4.47	10.90
Second proposed method	0.11	1.55	2.89	6.06

Lambertian fitting to model the relation distance-RSS and the multilateration to retrieve the position from the estimated distances. The second proposed method has a performance that is slightly inferior to that of the ANN method, but it has the advantage of being simpler.

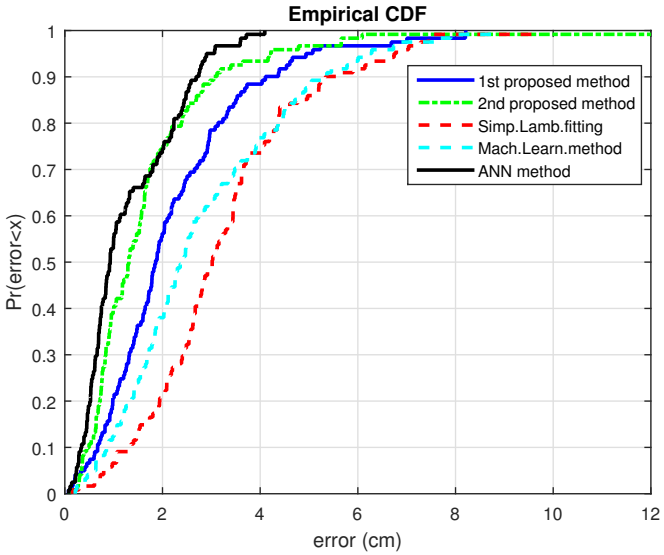

Fig. 4.10. CDF of the positioning errors obtained with the five VLP methods, using test file 2

From Figures 4.9 and 4.10, it can be observed that large errors may occur with the simplified Lambertian method and the machine learning method. It is the case also of the first proposed method with the second test file. However, we have observed that in this case these errors may be reduced if all the measurements are used for the training, instead of using only those taken at the 11 points lying on the diagonal (the maximum error is reduced from 10.90 cm to 8.21 cm). This is not the case for the simplified Lambertian method.

5. CONCLUSION

In this paper, we have proposed two new RSS-based VLP methods and compared their performances to that of three other methods from the literature. In the first method, we have proposed to replace the simplified Lambertian fitting used in [35] with an improved polynomial fitting. We have shown experimentally that this improvement in the fitting results in an improvement in the positioning accuracy. In the second method, we have proposed to estimate the coordinates of the mobile separately and directly from the received powers. We have applied surface fitting to learn the relation coordinates-received power. Since this type of fitting is limited to two variables, we have devised a technique that combines several coordinates estimates, each estimate being based on two powers among the four received

powers, taking into account the existence of two possible estimates for each couple of powers. We have shown that the performance of this method is comparable to that of the best method, which is the ANN method, while being simpler. It should be noted that by the same way we have validated experimentally the ANN method, which has been evaluated only by simulations in the original paper where it has been presented. It should also be highlighted that given that only standard low cost commercial components were used in our experimentation, the obtained positioning accuracy is very interesting.

REFERENCES

1. Cossu, G., Presi, M., Corsini, R., Choudhury, P., Khalid, A. M., et. al. (2011, December). A visible light localization aided optical wireless system. In *2011 IEEE GLOBECOM Workshops (GC Wkshps)* (pp. 802–807). IEEE.
2. Do, T. H., & Yoo, M. (2016). An in-depth survey of visible light communication based positioning systems. *Sensors*, **16**(5), 678.
3. Du, P., Zhang, S., Chen, C., Alphones, A., & Zhong, W. D. (2018). Demonstration of a low-complexity indoor visible light positioning system using an enhanced TDOA scheme. *IEEE Photonics Journal*, **10**(4), 1–10.
4. Eroglu, Y. S., Guvenc, I., Pala, N., & Yuksel, M. (2015, April). AOA-based localization and tracking in multi-element VLC systems. In *2015 IEEE 16th annual wireless and microwave technology conference (WAMICON)* (pp. 1–5). IEEE.
5. Fang, S. H., Wang, C. H., Huang, T. Y., Yang, C. H., & Chen, Y. S. (2012). An enhanced ZigBee indoor positioning system with an ensemble approach. *IEEE Communications Letters*, **16**(4), 564–567.
6. Guan, W., Huang, L., Wen, S., Yan, Z., Liang, W., et. al. (2021). Robot localization and navigation using visible light positioning and SLAM fusion. *Journal of Lightwave Technology*, **39**(22), 7040–7051.
7. Guan, W., Zhang, X., Wu, Y., Xie, Z., Li, J., et. al. (2019). High precision indoor visible light positioning algorithm based on double LEDs using CMOS image sensor. *Applied Sciences*, **9**(6), 1238.
8. Hsu, C. W., Liu, S., Lu, F., Chow, C. W., Yeh, C. H., et. al. (2018, March). Accurate indoor visible light positioning system utilizing machine learning technique with height tolerance. In *Optical Fiber Communication Conference* (pp. M2K-2). Optica Publishing Group.
9. Huang, C. H., Lee, L. H., Ho, C. C., Wu, L. L., & Lai, Z. H. (2014). Real-time RFID indoor positioning system based on Kalman-filter drift removal and Heron-bilateration location estimation. *IEEE Transactions on Instrumentation and Measurement*, **64**(3), 728–739.
10. Huang, H., Yang, A., Feng, L., Ni, G., & Guo, P. (2017). Artificial neural-network-based visible light positioning algorithm with a diffuse optical channel. *Chinese Optics Letters*, **15**(5), 050601.
11. Huynh, P., & Yoo, M. (2016). VLC-based positioning system for an indoor environment using an image sensor and an accelerometer sensor. *Sensors*, **16**(6), 783.
12. Jiang, J., Guan, W., Chen, Z., & Chen, Y. (2019). Indoor high-precision three-dimensional positioning algorithm based on visible light communication and fingerprinting using K-means and random forest. *Optical Engineering*, **58**(1), 016102–016102.
13. Jung, S. Y., Choi, C. K., Heo, S. H., Lee, S. R., & Park, C. S. (2013, January). Received signal strength ratio based optical wireless indoor localization using light emitting diodes for illumination. In *2013 IEEE International Conference on Consumer Electronics (ICCE)* (pp. 63–64). IEEE.
14. Jung, S. Y., Hann, S., & Park, C. S. (2011). TDOA-based optical wireless indoor localization using LED ceiling lamps. *IEEE Transactions on Consumer Electronics*,

57(4), 1592–1597.
15. Kim, H. S., Kim, D. R., Yang, S. H., Son, Y. H., & Han, S. K. (2012). An indoor visible light communication positioning system using a RF carrier allocation technique. *Journal of lightwave technology*, **31**(1), 134–144.
16. Kuo, Y. S., Pannuto, P., Hsiao, K. J., & Dutta, P. (2014, September). Luxapose: Indoor positioning with mobile phones and visible light. In *Proceedings of the 20th annual international conference on Mobile computing and networking* (pp. 447–458).
17. Kuriakose, J., Joshi, S., & George, V. I. (2014). Localization in wireless sensor networks: a survey. *arXiv*: 1410.8713, [Online]. Available: https://arxiv.org/abs/1410.8713
18. Le Minh, H., O'Brien, D., Faulkner, G., Zeng, L., Lee, K., et. al. (2009). 100-Mb/s NRZ visible light communications using a postequalized white LED. *IEEE Photonics Technology Letters*, **21**(15), 1063–1065.
19. Lin, P., Hu, X., Ruan, Y., Li, H., Fang, J., et. al. (2020). Real-time visible light positioning supporting fast moving speed. *Optics Express*, **28**(10), 14503–14510.
20. Liu, H., Darabi, H., Banerjee, P., & Liu, J. (2007). Survey of wireless indoor positioning techniques and systems. *IEEE Transactions on Systems, Man, and Cybernetics, Part C (Applications and Reviews)*, **37**(6), 1067–1080.
21. Nah, J. H. Y., Parthiban, R., & Jaward, M. H. (2013, October). Visible light communications localization using TDOA-based coherent heterodyne detection. In *2013 IEEE 4th international conference on photonics (ICP)* (pp. 247–249). IEEE.
22. Pau, G., Collotta, M., Maniscalco, V., & Choo, K. K. R. (2019). A fuzzy-PSO system for indoor localization based on visible light communications. *Soft Computing*, **23**, 5547–5557.
23. Rahman, M. S., Haque, M. M., & Kim, K. D. (2011). Indoor positioning by LED visible light communication and image sensors. *International Journal of Electrical and Computer Engineering*, **1**(2), 161.
24. Rida, M. E., Liu, F., Jadi, Y., Algawhari, A. A. A., & Askourih, A. (2015, April). Indoor location position based on bluetooth signal strength. In *2015 2nd International Conference on Information Science and Control Engineering* (pp. 769-773). IEEE.
25. Sahin, A., Eroglu, Y. S., Guvenc, I., Pala, N., & Yuksel, M. (2015, September). Accuracy of AOA-based and RSS-based 3D localization for visible light communications. In *2015 IEEE 82nd Vehicular Technology Conference (VTC2015-Fall)* (pp. 1-5). IEEE.
26. Sharifi, H., Kumar, A., Alam, F., & Arif, K. M. (2016, August). Indoor localization of mobile robot with visible light communication. In *2016 12th IEEE/ASME International Conference on Mechatronic and Embedded Systems and Applications (MESA)* (pp. 1–6). IEEE.
27. Sun, X., Zou, Y., Duan, J., & Shi, A. (2015, July). The positioning accuracy analysis of AOA-based indoor visible light communication system. In *2015 International Conference on Optoelectronics and Microelectronics (ICOM)* (pp. 186–190). IEEE.
28. Yang, C., & Shao, H. R. (2015). WiFi-based indoor positioning. *IEEE Communications Magazine*, **53**(3), 150–157.
29. Yang, S. H., Jung, E. M., & Han, S. K. (2013). Indoor location estimation based on LED visible light communication using multiple optical receivers. *IEEE Communications Letters*, **17**(9), 1834–1837.
30. Yang, S. H., Kim, H. S., Son, Y. H., & Han, S. K. (2014). Three-dimensional visible light indoor localization using AOA and RSS with multiple optical receivers. *Journal of Lightwave Technology*, **32**(14), 2480–2485.
31. Yasir, M., Ho, S. W., & Vellambi, B. N. (2014). Indoor positioning system using visible light and accelerometer. *Journal of Lightwave Technology*, **32**(19), 3306–3316.
32. Zhang, D., Xia, F., Yang, Z., Yao, L., & Zhao, W. (2010, May). Localization technologies for indoor human tracking. In *2010 5th international conference on future information technology* (pp. 1–6). IEEE.

33. Zhang, R., Zhong, W. D., Kemao, Q., & Zhang, S. (2017). A single LED positioning system based on circle projection. *IEEE Photonics Journal*, *9*(4), 1–9.
34. Zhang, W., & Kavehrad, M. (2012, July). A 2-D indoor localization system based on visible light LED. In *2012 IEEE photonics society summer topical meeting series* (pp. 80–81). IEEE.
35. Zheng, H., Xu, Z., Yu, C., & Gurusamy, M. (2017). A 3-D high accuracy positioning system based on visible light communication with novel positioning algorithm. *Optics Communications*, **396**, 160–168.
36. Zhou, Z., Kavehrad, M., & Deng, P. (2012). Indoor positioning algorithm using light-emitting diode visible light communications. *Optical engineering*, **51**(8), 085009–085009.
37. Zhuang, Y., Hua, L., Qi, L., Yang, J., Cao, P., et. al. (2018). A survey of positioning systems using visible LED lights. *IEEE Communications Surveys & Tutorials*, **20**(3), 1963–1988.

